Article

Synthesis, X-ray Crystal Structures, Computational Studies and Catechol Oxidase Activity of New Acylhydrazone Derivatives

Khalid Karrouchi [1,2,3], Smaail Radi [2,*], El bekkaye Yousfi [4], Nada Kheira Sebbar [5], Jamal Taoufik [1], Younes Ouzidan [6], Hazem A. Ghabbour [7,8], Yahia N. Mabkhot [9,*], Salim S. Al-Showiman[9] , Seham Alterary[9], M'hammed Ansar [1]

[1] Laboratoire de Chimie Thérapeutique, Faculté de Médecine et de Pharmacie, Université Mohammed V, Rabat, Morocco; Khalid.karrouchi@um5s.net.ma (K.K) ; jataoufik@hotmail.com (J.T) ; ansarmhammed@gmail.com (M.A)

[2] Laboratoire de Chimie Appliquée et Environnement (LCAE), Faculté des Sciences, Université Mohamed I, 60000 Oujda, Morocco; s.radi@ump.ac.ma ; radi_smaail@yahoo.fr (S.R)

[3] Laboratoire National de Contrôle des Médicaments, Direction du Médicament et de la Pharmacie, Ministère de la Santé, Rabat, Morocco;

[4] Institution Supérieure des Professions Infirmières et Techniques de Santé, Oujda, Morocco; yousfi@netcourrier.com (E.Y)

[5] Laboratoire de Chimie Organique Hétérocyclique, Pharmacochimie, Faculté des sciences, Université Mohammed V, Rabat, Morocco; snounousebbar@gmail.com (N.K.S)

[6] Laboratoire de Chimie Organique Appliquée, Faculté des Sciences et Techniques, Université Sidi Mohamed Ben Abdellah, Fès, Morocco; younes.ouzidan@usmba.ac.ma (Y.O)

[7] Department of Pharmaceutical Chemistry, College of Pharmacy, King Saud University, P. O. Box 2457, Riyadh 11451, Saudi Arabia; ghabbourh@yahoo.com (H.A.G)

[8] Department of Medicinal Chemistry, Faculty of Pharmacy, University of Mansoura, Mansoura 35516, Egypt. ghabbourh@yahoo.com (H.A.G)

[9] Department of Chemistry, Faculty of Science, King Saud University, P.O. Box 2455, Riyadh 11451, Saudi Arabia; yahia@ksu.edu.sa (Y.N.M), showiman@KSU.EDU.SA (S.S.A), salterary@KSU.EDU.SA(S.A)

* Correspondence: yahia@ksu.edu.sa; radi_smaail@yahoo.fr ; s.radi@ump.ac.ma; Tel.: +212-536-500-601.

Abstract: To make low-cost catalytic materials that mimic the activity of tyrosinase enzymes (Catechol oxidase) is an exciting challenge of biochemical technology. Herein, we report the synthesis of a series of acylhydrazone-pyrazoles based biomolecule materials (**L1-L7**) with superior catecholase activity. These biomolecules were synthesized by a one pot chemical condensation between 5-methyl-*1H*-pyrazole-3-carbohydrazide and benzaldehyde derivatives. The X-ray single crystal diffraction (XRD) for two ligands **L1** and **L2** have been studied and the molecular structures were optimized and confirmed using the density functional theory (DFT/B3LYP) method. Copper (II) complexes of the biomolecules (**L1-L7**), generated in-situ, and were studied for their catalytic activities towards the oxidation reaction of catechol to ortho-quinone according to two parameters: the nature of the ligand and the nature of counter anion. The **L7**-$CuSO_4$ was found to have an excellent catalytic activity (105.42 $\mu mol \cdot L^{-1} \cdot min^{-1}$) among the catalysts recently reported in the existing literature.

Keywords: Acylhydrazone; Pyrazole; X-ray crystallography; DFT/B3LYP; Catecholase activity.

1. Introduction

Copper has been known as an essential bioelement; its biological role(s) has been renowned only in the last decades due to: (i) the rapid evolution of bioinorganic chemistry, (ii) a succeed interaction between model complexes and (iii) protein biochemistry [1-4]. Especially, copper

Preprints (www.preprints.org) | NOT PEER-REVIEWED | Posted: 28 January 2018 doi:10.20944/preprints201801.0260.v1

containing metalloproteins have attracted a lot of attention in bioinorganic chemistry for their biological catalytic activity and their property of reversibly binding and activating dioxygen [5-8].

The oxidation of organic substrates with molecular oxygen under sweet conditions is of wide interest for industrial and synthetic processes both from a biochemical, economical and environmental point of view. The synthesis and investigation of functional model complexes for metalloenzymes with catechol oxygenase or catechol oxidase activity is therefore of great promise for the development of new and efficient catalysts for oxidation reactions [9]. Two major enzymes play the key role in these reactions, catechol dioxygenases and catechol oxidases. Most functional mimics of catechol oxidase are mono- or dinuclear Cu(II) complexes [10-15].

Accordingly, aroyl hydrazones are rather interesting as they present a combination of donor sites, such as a protonated/deprotonated amide oxygen atom, imine nitrogen atom of the hydrazone moiety and an additional donor site (usually N or O) provided from the aldehyde or ketone forming the Schiff base [16-19]. Nowadays, hydrazones form large variety of complexes with chemical, structural, biological and industrial importance [20-24].

On the other hand, pyrazole derived metal ion complexes have been widely studied in recent years owing to their high diversity of biological activity, ranging from antioxidant, antibacterial, antitumoral, and antiamoebic activities [25-30]. Great interest is also shown in catechol oxidase model complexes containing pyrazole ligands [31-35].

In continuation of our recent work in this field [36], we report herein the synthesis and the characterization of more active biomolecules based on new acylhydrazone-pyrazole ligands. DRX analysis, DFT calculations and catechol oxidase activity of the synthesized compounds were studied. All parameters that can affect the catalytic activity were investigated.

2. Results and discussion

2.1. *Synthesis and characterization*

The hydrazones described here were facilely synthesized according to the procedures outlined in Scheme 1. Commercially disposable aldehydes were refluxed in absolute ethanol with the 5-methyl-1H-pyrazole-3-carbohydrazide (**2**) during 2-5 h. The reaction was followed by TLC until completion. The solution was then cooled to room temperature and the resulting precipitate was collected by filtration to provide the corresponding hydrazones in excellent yield (Table 1).

The structures of all compounds were confirmed based on their spectroscopic data (^{1}H-NMR, ^{13}C-NMR, FT-IR, and ESI-MS).

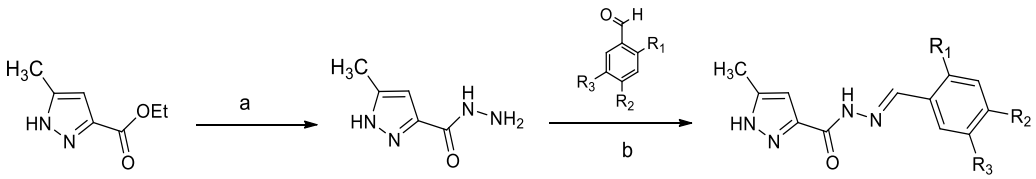

Scheme 1. The synthetic routes of compounds **L1-L7**, Reagents and conditions: (a) hydrazine hydrate (80%), ethanol, reflux 5h; (b) ethanol, acetic acid, reflux, 2-5 h.

Table 1. Synthesis and characterization data of the compounds **L1-L7.**

Compounds	R_1	R_2	R_3	Molecular formula	Mr (g/mol)	Yield (%)	M.p (°C)
L1	H	NO_2	H	$C_{12}H_{11}N_5O_3$	273.25	84	283-285
L2	Cl	H	H	$C_{12}H_{10}ClN_4O$	297.14	95	258-260
L3	H	Br	H	$C_{12}H_{10}BrN_4O$	307.15	80	300-302
L4	H	Cl	H	$C_{12}H_{10}ClN_4O$	262.69	64	301-303
L5	H	F	H	$C_{12}H_{10}FN_4O$	246.24	75	310-312

Preprints (www.preprints.org) | NOT PEER-REVIEWED | Posted: 28 January 2018 doi:10.20944/preprints201801.0260.v1

L6	OH	H	OCH_3	$C_{12}H_{11}BrN_4O_2$	323.15	63	254-256
L7	H	CH_3	H	$C_{13}H_{14}N_4O$	242.28	59	292-294

2.2. *X-Ray Crystal Structure Description*

The compounds **L1** and **L2** were analyzed by X-ray diffraction. Refinement parameters and crystal data are listed in Table 2. Supplementary data are deposited at CCDC under deposition numbers 1583324 and 1583326.

Figures 1 and 2 show the symmetric unit of **L1** and **L2**, respectively. The selected bond lengths and bond angles and hydrogen bonds are listed in Table S1 and S3 in the supplementary materials. All the bind lengths and angles are in normal ranges. In the crystal structures, the pyrazole ring (N1/N2/C2-C4) makes diheadral angle with the phenyl ring (C7-C12) 28.45° and 6.69° in **L1** and **L2**, respectively. The presence of the para nitro group in **L1** makes the phenyl ring more out of the plane of the pyrazole ring, in respect to the ortho chloro substitution in **L2**. In the crystal packing, **L1** molecules are linked via two intermolecular hydrogen bonds between N1—H1N1···O1i and C11—H11A···N2ii, Symmetry codes: (i) x, y−1, z; (ii) x−1, y+1, z (Table S2). On the other hand, the L2 molecules are arranged together by three hydrogen bonds between N3—H1N3···N2i, N1—H1N1···O1ii and C6—H6A···N2i, Symmetry codes: (i) −x+1, y, −z+3/2; (ii) x+1/2, −y+3/2, z+1/2 (Table S4).

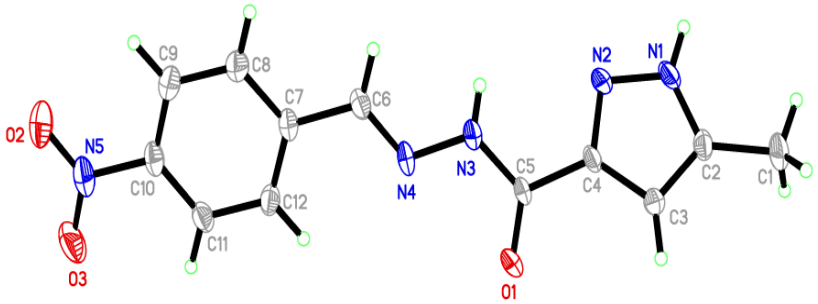

Figure 1. Asymmetric unit of **L1** (CCDC 1583324).

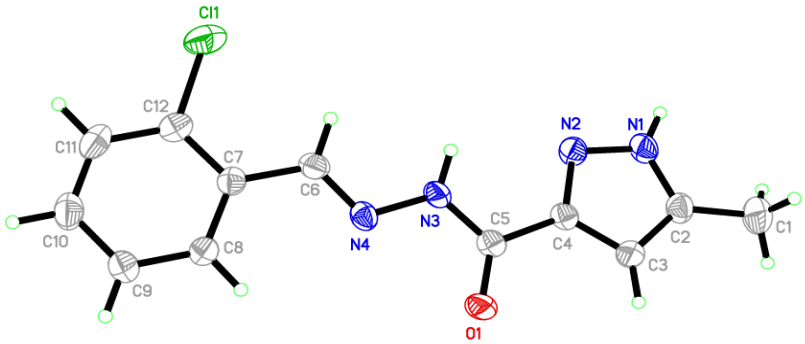

Figure 2. Asymmetric unit of **L2** (CCDC 1583326).

Table 2. Refinement parameters and crystal data for **L1** and **L2.**

CCDC Deposition Number	**L1:** 1583324	**L2:** 1583326
Molecular Formula	$C_{12}H_{11}N_5O_3$	$C_{12}H_{10}ClN_4O$
Molecular Weight	273.26	262.70
Crystal System	Triclinic	Monoclinic
Space Group	*P*1	*C*2/*c*

Preprints (www.preprints.org) | NOT PEER-REVIEWED | Posted: 28 January 2018 doi:10.20944/preprints201801.0260.v1

a (Å)	4.6957 (3)	12.6881 (14)
b (Å)	7.2287 (4)	16.905 (2)
c (Å)	9.8261 (7)	13.073 (2)
α (°)	104.084 (3)	90.0
β (°)	90.848 (3)	115.330 (4)
γ (°)	107.980 (3)	90.0
V (Å^3)	306.25 (3)	2534.6 (6)
Z	1	8
D_{calc} (Mg·m^{-3})	1.482	1.377
Crystal Dimension (mm)	0.31 × 0.29 × 0.14	0.55 × 0.14 × 0.13
μ (mm^{-1})	0.11	0.30
T_{min}/T_{max}	0.966, 0.984	0.855, 0.963
Measured Reflections	10086	27408
Indices Range (h, k, l)	−6/6, −9/9, −12/12	−16/16, −21/21, −16/16
θ Limit (°)	2.2-27.5	2.2-27.5
Unique Reflections	2795	2912
Parameters	190	172
Goodness of Fit on F^2	1.04	1.02
R_1,wR_2 [I > 2σ(I)]	0.0572, 0.124	0.0546, 0.141

2.3. *Computational studies*

The optimized geometry of compounds **L1** and **L2** were been obtained at B3LYP/6-31G* level. Some optimized geometric parameters are also listed in Figure 3 and Tables 3, 4 and 5.

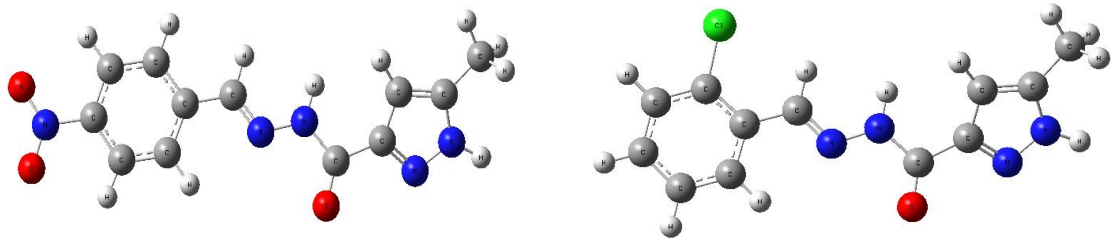

L1 **L2**

Figure 3. Optimized geometry of **L1** and **L2**.

The actual and optimized bond lengths and bond angles obtained by X-ray crystallographic study as well as by geometry optimization at B3LYP/6-31G level of theory of structure **L1** and **L2** are reported in Table 4 and table 5 succefly.

In case of X-ray structure of compound **L1**, the observed bond lengths of N1-N2, N1-C2 and N2-C4 bonds in five membered pyrazole ring are 1.340 (3) Å, 1.338 (4) Å and 1.327 (4) Å respectively. The calculated bond lengths, through DFT method, of same pyrazole ring, are 1.342Å, 1.364Å and 1.335Å respectively, which are very close to the actual values. From Table 2, it is clear that actual C-C and C-H bond lengths are also in close agreement with calculated values. The calculated bond angles for N2N1C2, N4N3C5 and O1C5N3 bond angles of **L1** are 114.34, 120.66and 123.16° respectively, which are close to corresponding actual angles obtained from X-ray. The actual values of above bond angles are 113.7 (2), 119.4 (2) and 123.3 (2) ° respectively.

In case of X-ray structure of compound **L2**, the observed bond lengths of Cl1-C12, O1-C5 and N2-C4 in the pyrazole derivative are 1.738 (3) Å, 1.219 (3) Å and 1.332 (3) Å respectively. The

Preprints (www.preprints.org) | NOT PEER-REVIEWED | Posted: 28 January 2018 doi:10.20944/preprints201801.0260.v1

calculated bond lengths, through DFT method, of same bond lengths, are 1.768Å, 1.213Å and 1.335Å respectively, which are very close to the actual values. The calculated bond angles for N2N1C2, N1N2C4 and O1C5N3 bond angles of **L2** are 114.31, 104.03 and 123.49° respectively, which are close to corresponding actual angles obtained from X-ray. The actual values of above bond angles are 113.1 (2), 103.9 (2) and 123.6 (2)° respectively (Table 4).

Table 3. Selected structural parameters by X-ray and theoretical calculations of **L1**.

Bond Length (Å)	Experimental Bond Lengths	Calculated Bond Lengths	Bond Angle (°)	Experimental Bond Angles	Calculated Bond Angles
O1—C5	1.213 (3)	1.212	N2—N1—C2	113.7 (2)	114.34
O2—N5	1.213 (4)	1.231	N1—N2—C4	103.5 (2)	104.01
O3—N5	1.224 (4)	1.232	N4—N3—C5	119.4 (2)	120.66
N1—N2	1.340 (3)	1.342	N3—N4—C6	116.8 (2)	118.00
N1—C2	1.338 (4)	1.364	O2—N5—O3	123.9 (3)	124.56
N2—C4	1.327 (4)	1.335	N2—C4—C3	112.2 (3)	111.35
N3—N4	1.360 (3)	1.346	N2—C4—C5	120.8 (2)	119.04
N3—C5	1.360 (3)	1.401	N3—C5—C4	115.2 (2)	112.12
N4—C6	1.275 (3)	1.285	O1—C5—N3	123.3 (2)	123.16
N5—C10	1.471 (4)	1.468	O1—C5—C4	121.6 (2)	124.71

Table 4. Selected structural parameters by X-ray and theoretical calculations of **L2**.

Bond Length (Å)	Experimental Bond Lengths	Calculated Bond Lengths	Bond Angle (°)	Experimental Bond Angles	Calculated Bond Angles
Cl1—C12	1.738 (3)	1.768	N2—N1—C2	113.1 (2)	114.31
O1—C5	1.219 (3)	1.213	N1—N2—C4	103.9 (2)	104.03
N1—N2	1.350 (3)	1.344	N4—N3—C5	118.9 (2)	120.82
N1—C2	1.348 (4)	1.364	N3—N4—C6	115.0 (2)	117.39
N2—C4	1.332 (3)	1.335	N2—C4—C5	122.0 (2)	119.08
N3—N4	1.380 (3)	1.351	N3—C5—C4	115.3 (2)	112.11
N3—C5	1.350 (3)	1.397	O1—C5—N3	123.6 (2)	123.49
N4—C6	1.275 (3)	1.285	O1—C5—C4	121.1 (2)	124.40

The total energy, energy of HOMO and energy of LUMO, as well as other parameters for structures **L1** and **L2** are obtained theoretically and listed in Table 5. The HOMO and LUMO electrons density distributions of **L1** and **L2** are given in (Figure 4 and 5). After the analysis of the theoretical results obtained, we can say that the molecules **L1** and **L2** have a non-planar structure.

The analysis of the wave function indicates that the energy space between the molecular orbit HOMO and LUMO determines the chemical stability and the electrical transport properties of the molecule. The red and green colors of the molecular orbital ridge respectively represent the positive and negative phases. The HOMO of **L1** shows the charge density localized on the 4-nitrobenzaldehyde ring, but LUMO is characterized by a charge distribution on the hydrazone function, indicating that this moiety can influence the electron transition. The HOMO of **L2** has a

Preprints (www.preprints.org) | NOT PEER-REVIEWED | Posted: 28 January 2018 doi:10.20944/preprints201801.0260.v1

localized charge density on the pyrazole and hydrazone function, but LUMO is characterized by a charge distribution on the 2-chlorobenzaldehyde ring and the hydrazone function. The energy difference between HOMO and LUMO of **L1** and **L2** is about 3.04 and 6.01 eV respectively. The energy of the smaller band space increases the stability of the molecule. The molecular boundary orbitals of **L1** and **L2** (HOMO-LUMO) are shown in Figures 4 and 5.

Table 5. Calculated energies of **L1** and **L2**.

Molecular Energy(a.u)	L1	L2
TE **(eV)**	-26209.0	-33150.1
E_{HOMO}**(eV)**	-6.5021	-6.2047
E_{LUMO}**(eV)**	-3.4611	-0.1918
Gap ΔE**(eV)**	3.0410	6.0129
μ**(D)**	11.2421	5.3366

We also studied the HOMO-LUMO gap of **L1** and **L2** to discover their reactivity towards the catechol oxidation reaction. We found that the complex formed in-situ with **L1** (3.04 eV) has a lower HOMO-LUMO difference compared to the **L2** complex (6.01 eV). It proves that the ligand **L2** is more reactive with respect to the oxidation of catechol with respect to the ligand **L1**. On the other hand, the calculated HOMO energies are respectively -6.50, -6.20 eV for the ligand L1 and L2. It shows that the HOMO orbital is strongly stabilized in **L2** and ready to accept an electron, which facilitates the catechol oxidation reaction. Thus, the oxidation tendency of catechol (**L2>L1**) is very consistent with our experimental observation.

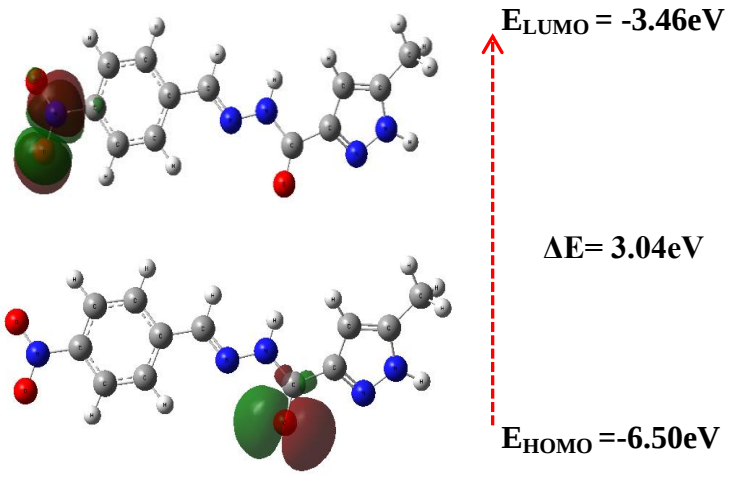

Figure 4. HOMO-LUMO energy diagram of **L1.**

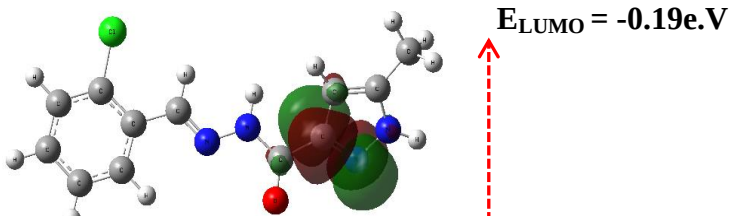

Preprints (www.preprints.org) | NOT PEER-REVIEWED | Posted: 28 January 2018 doi:10.20944/preprints201801.0260.v1

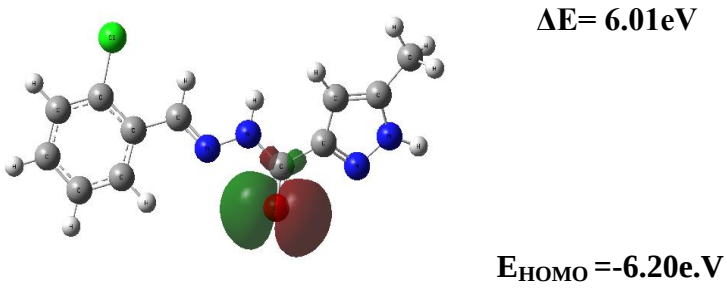

Figure 5. HOMO-LUMO energy diagram of **L2**.

2.4. *Catecholase activity: spectrophotometric study*

The catechol oxidation reaction catalysed by the different copper complexes is studied by following the concentration of O-quinone produced using a UV-Vis spectrometer. This study is performed by monitoring the high absorption peak of o-quinone resulting from the catalyzed reaction (Scheme 2). The copper complex is obtained in situ [31] by mixing the copper salt and the ligand just before the introduction of the catechol solution. All of these solutions are placed together in the spectrophotometer cell at 25 ° C. Thus, the formation of o-quinone is followed by the increase of the absorbance at 390 nm as a function of time (Figure 6).

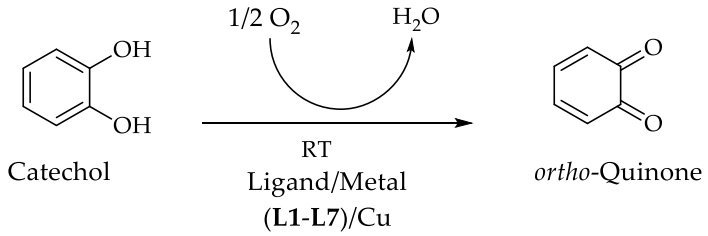

Scheme 2. Catecholase reaction.

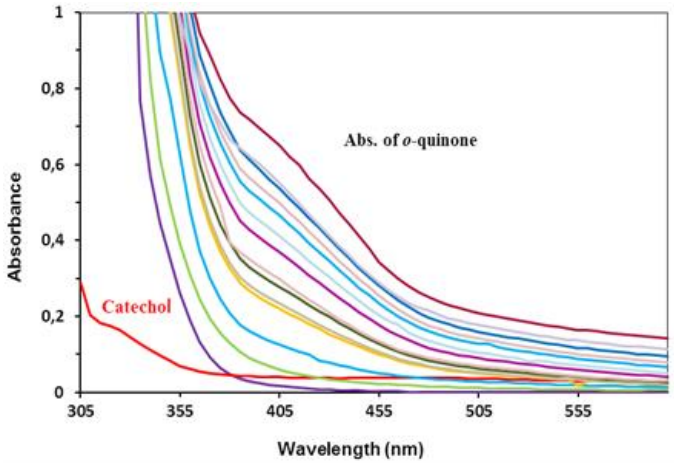

Figure 6. Increase of *o*-quinone band at 390 nm after addition of **L3** and $CuSO_4$.

The variation of the absorbance as a function of time for each ligand and with different copper salts is presented in the curves of Figure 7.

Preprints (www.preprints.org) | NOT PEER-REVIEWED | Posted: 28 January 2018 doi:10.20944/preprints201801.0260.v1

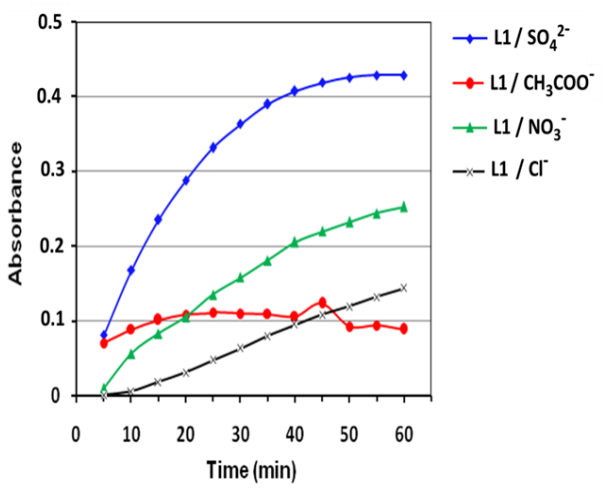

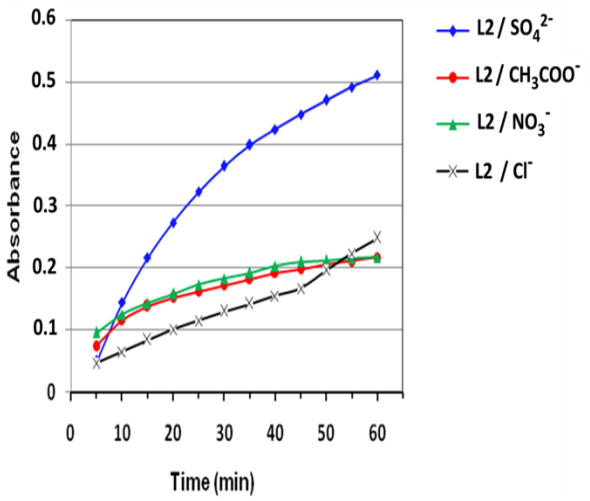

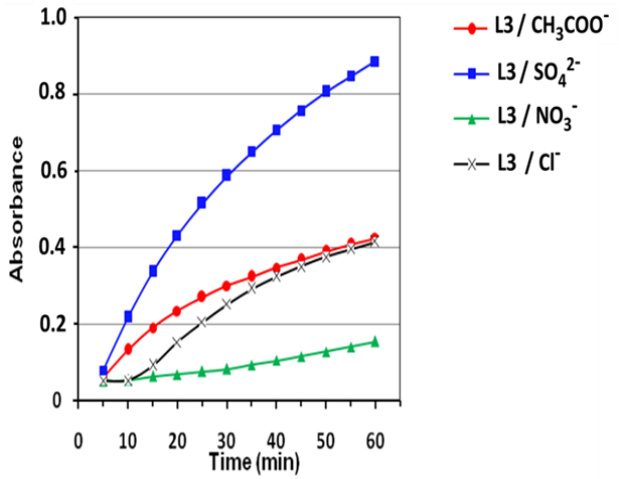

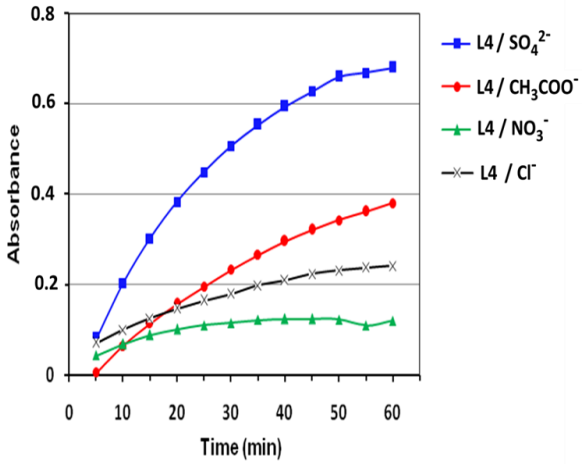

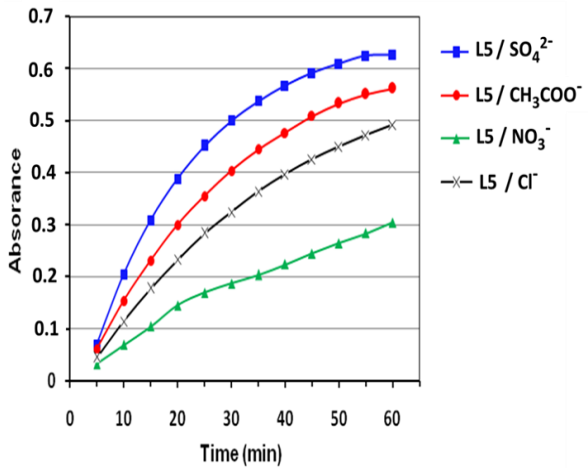

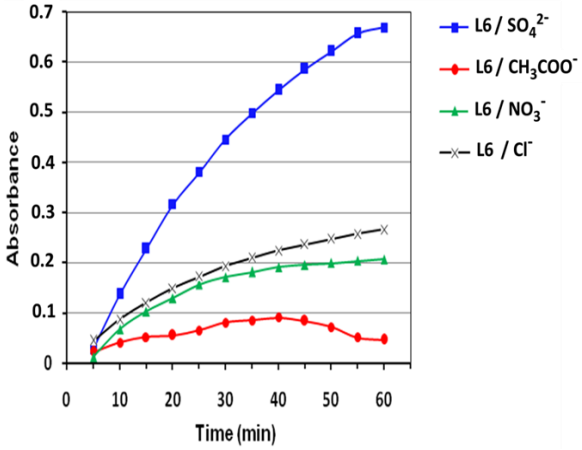

Preprints (www.preprints.org) | NOT PEER-REVIEWED | Posted: 28 January 2018 doi:10.20944/preprints201801.0260.v1

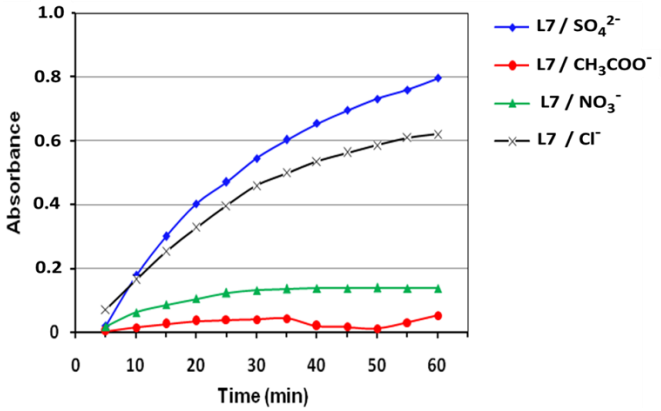

Figure 7. Plot of absorbance vs time for the oxidation of catechol catalyzed by copper complexes formed with different ligands (**L1-L7**) and copper salts.

All cures exhibit an increasing absorbance in the time indicating that all of ligands are catecholase activity. On the other hand, we can note that the curves are not exactly identical which shows a difference in the catalytic activity.

The calculated catecholase activity of differentes ligands with different copper salts were presented in Table 6.

Table 6. Catecholase activity of complexes in methanol ($\mu mol.L^{-1}.min^{-1}$) with different copper salts.

Ligand / Metallic salt	$Cu(NO_3)_2$	$CuCl_2$	$Cu(CH_3COO)_2$	$CuSO_4$
L1	23.96	9.59	9.59	62.29
L2	19.17	14.38	23.96	67.09
L3	4.79	43.13	47.92	**100.63**
L4	9.59	19.17	43.13	**95.84**
L5	33.54	52.71	67.09	**100.63**
L6	28.75	23.96	9.59	81.46
L7	19.17	76.67	4.79	**105.42**

From the results of the Table 6, we can note that all the ligands have a considerable catalytic activity. Indeed, a maximum activity of about 100 ± 5 $\mu mol.L^{-1}.min^{-1}$ is obtained for the **L3**[$CuSO_4$], **L4**[$CuSO_4$], **L5**[$CuSO_4$] and **L7**[$CuSO_4$] complexes. Low activity values of 4.79 $\mu mol.L^{-1}.min^{-1}$ are obtained for the **L3**[$Cu(NO_3)_2$] and **L7**[$Cu(CH_3COO)_2$] complexes. The rate of oxidation appears to be influenced by the ligand and copper salt parameters. The effect of ligand nature on oxidation rate is less important for $Cu(NO_3)_2$ salt because mean absolute deviation is lower than 7.6. However, in the cases of $CuCl_2$ and $Cu(CH_3COO)_2$, the effect is more important because mean absolute deviation is quite high than 19.9.

The effect of changing the copper salts on the oxidation rate is not the same for different ligands. The salt which gives the highest reaction rate is $CuSO_4$ salt and the one which gives the lowest rate is $Cu(NO_3)_2$. The effect of the copper salt can be explained by a difficulty in the formation of the L[Cu] complex. Indeed, ions such as NO_3^- and CH_3OO^- can form stronger bonds with Cu^{2+} which can prevent the formation of complexes.

The ligand **L2** with a radical (Cl) in position (R1) ortho of the phenyl gives an activity lower than the ligand **L4** which has a radical (Cl) in position (R2) para of the phenyl. This result can be explained by a steric hindrance effect of the radical in the position (R1) ortho and which can prevent the formation of the copper complex. It is also possible that the formed complex has a geometry that is not adapted to the substrate. We can notice the same observation for the ligand **L6** which gives a low rate reaction since it also has an (OH) radical in the ortho position of the phenyl.

Preprints (www.preprints.org) | NOT PEER-REVIEWED | Posted: 28 January 2018 doi:10.20944/preprints201801.0260.v1

The **L3**, **L4** and **L5** ligands differ by the R2 radical, such as Cl, Br and F respectively. It is noted that, with the exception of **L5**, the **L3** and **L4** ligands give similar activities. These activities remain lower than those obtained by **L5**. This difference may be due to the electronegativity values of these halogens. On the one hand for fluoride, the high electronegativity gives a better activity of the complex. On the other hand, Cl and Br have neighboring electronegativities that give similar activities. This is explained by the stability of the ligands by mesomeric effect in the case of electronegative radicals.

2.5. Comparison with Alternative Catalysts

Table 7 attests the catalytic activity by recent catalysts reported in the literature. It is clear that the acylhydrazone-pyrazole derivatives, in particular ligand **L7**, described in this work present better values and higher activity for the effective aerobic oxidation of the catechol into o-quinone. To our knowledge, the catalytic activity observed for ligand **L7** (105.42 $\mu mol.L^{-1}.min^{-1}$) is the most important among the catalysts described in the literature. This best catalytic activity is probably due to the stability of corresponding copper complex (catalyst) favored by the intense coordination bonds of the Schiff base.

Table 7. Comparison of the catalytic activity of various catalysts toward oxidation of the catechol into o-quinone, established in the same conditions, as given in previous literature.

Cu(II)-Ligands	Cu(II) Salt Used	Oxidation Rate ($\mu mol \cdot L^{-1} \cdot min^{-1}$)	Ref.
Ligand **L7**	$CuSO_4$	**105.42**	-
bipyrazolic tripode-3-hydroxypropyl	$CuCl_2$	4.378	[31]
bipyrazolic tripode-4-hydroxyphenyl	$CuCl_2$	1.458	[32]
C,N-bipyrazole	$Cu(CH_3COO)_2$	4.440	[34]
(3,5-dimethyl-pyrazol-1-ylmethyl)-amino]-propionitrile	$CuSO_4$	8.710	[35]
N′-(diphenylmethylene)-5-phenyl-1H-pyrazole-3-carbohydrazide	$CuSO_4$	72.920	[36]
bipyrazolic tripode-prop-2-ylacetate	$Cu(CH_3COO)_2$	11.825	[37]
bipyrazolic tripode-3-hydroxypropyl	$CuSO_4$	28.990	[38]
indole-3-chalcone	$Cu(CH_3COO)_2$	31.780	[39]

3. Conclusions

In this work, we report the synthesis of seven new acylhydrazone-pyrazoles based biomolecule materials (**L1-L7**), with superior catecholase activity, in excellent yields. **L1** and **L2** structures were investigated by X-ray single crystal diffraction (XRD). The theoretical calculations of **L1** and **L2** through the density functional theory (DFT/B3LYP) method well supported the experimental findings. Ligands (**L1–L7**) and different Cu(II) salts demonstrate an efficient activity to catalyze the aerobic oxidation of the catechol into o-quinone compared to others recent catalysts described in the literatures. Interestingly, ligand L7 exhibits an extremely high rate of oxidation, attaining 105.42 $\mu mol.L^{-1}.min^{-1}$, which is, to our knowledge, the best catalytic activity among the reported catalysts. Cu(II) ligand complexes were generated in-situ and the results obtained show that the oxidation depend highly on two parameters: the nature of the ligand and the nature of salts. The results suggest that these new materials have potential for the oxidation of the catechol into o-quinone, thus opening important perspectives.

4. Experimental Section

4.1. Materials and physical measurements

 doi:10.20944/preprints201801.0260.v1

Melting points were measured using a Büchi B-545 digital capillary melting point apparatus and used without correction. Reactions were checked with TLC using aluminum sheets with silica gel 60 F254 from Merck. UV-visible (UV-vis) absorption spectra were recorded using a Perkin Elmer Lambda 35 ES UV/VIS spectrophotometer using quartz cuvettes of 1 cm pathlength. Spectra IR were recorded on a Perkin-Elmer VERTEX 70 FT-IR spectrometer covering field 400-4,000 cm^{-1}. The spectra of ^{1}H NMR and ^{13}C NMR were recorded in solution in DMSO-d_6 on a Bruker spectrometer (300 MHz). The chemical shifts are expressed in parts per million (ppm) by using tetramethylsilane (TMS) as internal reference. The multiplicities of the signals are indicated by the following abbreviations: s, singlet; d, doublet; t, triplet; q, quadruplet; and m, multiplet, and coupling constants are expressed in Hertz. Mass spectra were collected using an AB Sciex API 3200 LC/MS/MS system, equipped with an ESI source. The chemical reagents used in synthesis were purchased from Fluka, Sigma and Aldrich.

4.2. Synthesis

The synthesis of the intermediate and target compounds was performed according to the reactions outlined in Scheme 1. The new ligands (**L1-L7**) were synthesized and characterized according to the reported literature method [36, 40, 41].

General procedure for the preparation of N'-[(aryl)methylene]-5-methyl-1H-pyrazole-4-carbohydrazides (**L1-L7**): To a solution of 5-methyl-*1H*-pyrazole-3-carbohydrazide (**2**) (1 mmol) in 10 mL of ethanol was added an equimolar amount of the appropriate benzaldehyde derivative in the presence of acetic acid. The mixture was maintained under reflux for 2 h, until TLC indicated the end of reaction. Then, the reaction mixture was poured in cold water, and the precipitate formed was filtered out washed with ethanol and recrystallized from ethanol.

*N'-(4-nitrobenzylidene)-5-methyl-1H-pyrazole-3-carbohydrazide (**L1**):* Yield 84% (solid), M.p. 283-285°C; IR (ATR, ν(cm^{-1})) : 3320 (NH), 1681 (C=O), 1512 (N=CH) ; ^{1}H-NMR (300 MHz, DMSO-d_6, δ(ppm)): δ = 2.28 (s,3H, CH_3), 6.44 (s, 1H, H-pyrazole), 7.90 (d, J = 8.7 Hz, 2H, H-Ar), 8.27 (d, , J = 8.7 Hz, 2H, H-Ar), 8.58 (s, 1H, -CONH),11. 92 (s, 1H, N=CH), 13.13 (s, 1H, NH-pyrazole); ^{13}C NMR: (300MHz, DMSO-d_6, δ (ppm)): 10.77 (CH_3), 105.52 (CH, C4-pyrazole), 124.25 (CH, C3-Ar), 128.33 (CH, C2-Ar), 140.71 (C, C1-Ar), 141.40 (C, C3-pyrazole), 145.11 (CH, N=CH), 146.01 (C, C5-pyrazole), 148.14 (C, C-NO_2).; 159.10 (C, C=O); MS: m/z = 274.1 $(M+H)^+$.

*N'-(2-chlorobenzylidene)-5-methyl-1H-pyrazole-3-carbohydrazide (**L2**):* Yield 78%, M.p. 258-260°C; IR (ATR, ν(cm^{-1})) : 3182 (NH), 1665 (C=O), 1552 (N=CH) ; ^{1}HNMR (300 MHz, DMSO-d_6, δ(ppm)): δ = 2.27 (s, 3H, CH_3), 6.49 (s, 1H, H-pyrazole), 7.39 - 7.99 (m, 4H, H-pyrazole), 8.90 (s, 1H, -N=CH), 11. 92 (s, 1H, -CONH), 13.09 (s, 1H, NH-pyrazole) ; ^{13}C NMR: (300MHz, DMSO-d_6, δ (ppm)): 10.77 (CH_3), 105.40 (CH, C4-pyrazole), 127.31 (CH, C5-Ar), 128.01 (CH, C6-Ar), 130.34 (C, C3-Ar), 131.70 (C, C4-Ar), 132.41 (C, C1-Ar), 133.57 (C, C2-Ar), 140.56 (C, C3-pyrazole), 143.65 (CH, N=CH), 146.16 (C, C5-pyrazole), 159.05 (C, C=O); MS: m/z = 263.1 $(M+H)^+$.

*N'-(4-bromobenzylidene)-5-methyl-1H-pyrazole-3-carbohydrazide (**L3**):* Yield 80 %, M.p. 300-302 °C; IR (ATR, ν(cm^{-1})) : 3296 (NH), 1677 (C=O), 1617 (N=CH); ^{1}H-NMR (300 MHz, DMSO-d_6, δ(ppm)): δ = 2.26 (s,3H, CH_3), 6.49 (s, 1H, H-pyrazole), 7.42 (d, J = 8.7 Hz, 2H, H-Ar), 7.61 (d, J = 8.7 Hz, 2H, H-Ar), 8.45 (s, 1H, CONH), 11.67 (s, 1H, N=CH) 13.09 (s, 1H, NH-pyrazole) ; ^{13}C NMR: (300MHz, DMSO-d_6, δ (ppm)): 10.76 (CH_3), 105.36 (CH, C4-pyrazole), 123.48 (CH, C3-Ar), 129.28 (CH, C2-Ar),

 doi:10.20944/preprints201801.0260.v1

132.28 (C, C1-Ar), 134.32 (C, C4-Ar), 140.57 (C, C3-pyrazole), 146.27 (CH, N=CH), 146.36 (C, C5-pyrazole), 158.91 (C, C=O). MS: m/z = 308.1 $(M+H)^+$.

*N'-(4-chlorobenzylidene)-5-methyl-1H-pyrazole-3-carbohydrazide (**L4**):* Yield 64 %, M.p. 301-303 °C; IR (ATR, ν(cm^{-1})) : 3397 (NH), 1677 (C=O), 1618 (N=CH); ^{1}H-NMR (300 MHz, DMSO-d_6, δ(ppm)): δ = 2.27 (s,3H, CH_3), 6.49 (s, 1H, H-pyrazole), 7.47 (d, J = 8.7 Hz, 2H, H-Ar), 7.68 (d, J = 8.7 Hz, 2H, H-Ar), 8.45 (s, 1H, CONH), 11.67 (s, 1H, N=CH) 13.09 (s, 1H, NH-pyrazole) ; ^{13}C NMR: (300MHz, DMSO-d_6, δ (ppm)): 10.77 (CH_3), 105.35 (CH, C4-pyrazole), 129.04 (CH, C3-Ar), 129.37 (CH, C2-Ar), 133.98 (C, C1-Ar), 134.70 (C, C4-Ar), 140.57 (C, C3-pyrazole), 146.27 (CH, N=CH), 147.23 (C, C5-pyrazole), 158.91 (C, C=O). MS: m/z = 263.2 $(M+H)^+$.

*N'-(4-fluorobenzylidene)-5-methyl-1H-pyrazole-3-carbohydrazide (**L5**):* Yield 75 %, M.p. 310-312 °C; IR (ATR, ν(cm^{-1})) : 3336 (NH), 1677 (C=O), 1619 (N=CH); ^{1}H-NMR (300 MHz, DMSO-d_6, δ(ppm)): δ = 2.27 (s,3H, CH_3), 6.48 (s, 1H, H-pyrazole), 7.47 (d, J = 8.7 Hz, 2H, H-Ar), 7.68 (d, J = 8.7 Hz, 2H, H-Ar), 8.46 (s, 1H, CONH), 11.59 (s, 1H, N=CH) 13.07 (s, 1H, NH-pyrazole) ; ^{13}C NMR: (300MHz, DMSO-d_6, δ (ppm)): 10.77 (CH_3), 105.31 (CH, C4-pyrazole), 116.19 (CH, C3-Ar), 129.50 (CH, C2-Ar), 131.63 (C, C1-Ar), 140.55 (C, C3-pyrazole), 146.28 (CH, N=CH), 158.89 (C, C5-pyrazole), 161.80 (C, C=O), 165.08 (C, C4-Ar). MS: m/z = 247.1 $(M+H)^+$.

*N'-(4-hydroxy-3-methoxybenzylidene)-5-methyl-1H-pyrazole-3-carbohydrazide (**L6**):* Yield 65 %, M.p. 226-228 °C; IR (ATR, ν(cm^{-1})) : 3483 (OH), 3258 (NH), 1648 (C=O), 1590 (N=CH); ^{1}H-NMR (300 MHz, DMSO-d_6, δ(ppm)): δ = 2.26 (s,3H, CH_3), 3.80 (s,3H, OCH_3), 6.46 (s, 1H, H-pyrazole), 6.80 (d, J = 8.1 Hz, 1H, H-Ar), 7.00 (d, J = 8.1 Hz, 1H, H-Ar), 7.26 sd, 1H, H-Ar), 8.33 (s, 1H, CONH), 9.51 (s, 1H, OH), 11.38 (s, 1H, N=CH) 13.03 (s, 1H, NH-pyrazole) ; ^{13}C NMR: (300MHz, DMSO-d_6, δ (ppm)): 10.77 (CH_3), 56.00 (OCH_3), 105.20 (CH, C4-pyrazole), 109.20 (CH, C6-Ar), 115.86 (CH, C3-Ar), 122.43 (CH, C2-Ar), 126.42 (C, C1-Ar), 148.20 (C, C3-pyrazole), 148.47 (CH, N=CH), 149.23 (C, C5-pyrazole), 149.85 (C, OCH_3), 158.91 (C, OH), 158.91 (C, C=O). MS: m/z = 257.1 $(M+H)^+$.

*5-methyl-N'-(4-methylbenzylidene)-1H-pyrazole-3-carbohydrazide (**L7**):* Yield 59 %, M.p. 292-294 °C; IR (ATR, ν(cm^{-1})) : 3224 (NH), 1654 (C=O), 1606 (N=CH); ^{1}H-NMR (300 MHz, DMSO-d_6, δ(ppm)): δ = 2.26 (s,3H, CH_3), 2.31 (s, 3H, CH_3), 6.50 (s, 1H, H-pyrazole), 7.23 (d, J = 8.1 Hz, 2H, H-Ar), 7.55 (d, J = 8.1 Hz, 2H, H-Ar), 8.42 (s, 1H, -NH), 11.98 (s, 1H, N=CH) 13.10 (s, 1H, NH-pyrazole) ; ^{13}C NMR: (300MHz, DMSO-d_6, δ (ppm)): 11.06 (CH_3), 21.48 (CH_3), 105.27 (CH, C4-pyrazole), 127.42 (CH, C2-Ar), 129.88 (CH, C3-Ar), 132.28 (C, C1-Ar), 140.13 (C, C1-Ar), 141.73 (C, C3-pyrazole), 146.95 (CH, N=CH), 147.13 (C, C5-pyrazole), 158.80 (C, C=O). MS: m/z = 243.1 $(M+H)^+$.

4.3. X-ray Crystallographic Analysis

The compounds of **L1** and **L2** were obtained as single crystals by slow evaporation from ethanol solution of the pure compound at room temperature. Data were collected on a Bruker APEX-II D8 Venture area diffractometer, equipped with graphite monochromatic Mo Kα radiation, λ = 0.71073 Å at 296 (2) K, respectively. Cell refinement and data reduction were carried out by Bruker SAINT. SHELXT was used to solve structure [42, 43]. The final refinement was carried out by full-matrix least-squares techniques with anisotropic thermal data for no hydrogen atoms on *F*. CCDC 1583324 and 1583326 for **L1** and **L2**, respectively. The supplementary crystallographic data for these compounds can be obtained free of charge from the Cambridge Crystallographic Data Centre via www.ccdc.cam.ac.uk/data_request/cif.

4.4. DFT computational method

The computational studies of compounds **L1** and **L2** were performed at the B3LYP/6-31G level of theory using Gaussian 09 package programs [44, 45]. The optimizations geometries of **L1** and **L2** were performed using the Berny analytical gradient optimization method [46].

4.5. Catecholase activity measurement

Kinetic measurements were made spectrophotometrically on UV-Vis spectrometer, following the appearance of o-quinone over time at 25 °C (390 nm absorbance maximum ε = 1600 $L.mol^{-1}.cm^{-1}$ in methanol [33]. The complexes were prepared in-situ by successively mixing 0.15 mL of a solution (2×10^{-3} M) of CuX_2, nH_2O (X = Cl^-, NO_3^-, CH_3COO^- or SO_4^-), with 0.15 mL of a solution (2×10^{-3} M) of ligand, then adding 2 mL of a solution of catechol at a concentration of 10^{-1} M.

Supplementary Materials: The following are available online at www.mdpi.com/link, Table S1: Selected geometric parameters (Å, °) for **L1**, Table S2: Hydrogen-bond geometry (Å, °) for **L1**, Table S3: Selected geometric parameters (Å, °) for **L2**, Table S4: Hydrogen-bond geometry (Å, °) For **L2**.

Acknowledgments: The authors extend their appreciation to the Deanship of Scientific Research at King Saud University for funding this work through research group No. (RGP-007). Sincere appreciation is also extended to the PPR2-MESRSFC-CNRST-P10 project (Morocco).

Author Contributions: K. K., S. R. and M. A. carried out of the experimental work, performed the structural analysis and cooperated in the preparation of the manuscript. N. K. S. and Y. O. performed the density functional theory calculations. E. Y. carried out the catalytic activity. J. T. cooperated in the preparation of the manuscript and interpretation of the results. Y. N. M. and H. A. G. determined the X-ray crystal structure and Y. N. M also paid the publication fees.

Conflicts of Interest: The authors declare no conflict of interest.

References

1. Binolfi, A.; Quintanar, L.; Bertoncini, C. W.; Griesinger, C.; Fernández, C. O. Bioinorganic chemistry of copper coordination to alpha-synuclein: Relevance to Parkinson's disease. Coord. Chem. Rev. 2012, 256, 2188-2201, https://doi.org/10.1016/j.ccr.2012.05.004.
2. Chanu, O. B.; Kumar, A.; Lemtur, A.; Lal, R. A. Synthesis and characterization of homotrimetallic copper complexes derived from bis(2-hydroxy-1-naphthaldehyde)oxaloyldihydrazone. Spectroc. Acta A. 2012, 96, 854-861, https://doi.org/10.1016/j.saa.2012.07.113.
3. Kern, T.; Monkowius, U.; Zabel, M.; Knör, G. Synthesis, crystal structure and charge transfer spectra of dinuclear copper(I) complexes bearing 1,2-bis(arylimino)acenaphthene acceptor ligands. Inorg. Chim. Acta. 2011, 374, 632-636, https://doi.org/10.1016/j.ica.2011.02.042.
4. Shokohi-pour, Z.; Chiniforoshan, H.; Momtazi-borojeni, A. A.; Notash, B. A novel Schiff base derived from the gabapentin drug and copper (II) complex: Synthesis, characterization, interaction with DNA/protein and cytotoxic activity. J. Photochem. Photobiol. B. 2016, 162, 34-44, https://doi.org/10.1016/j.jphotobiol.2016.06.022.
5. Holland, P. L.; Tolman, W. B. A structural model of the type 1 copper protein active site: N2S (thiolate) S (thioether) ligation in a Cu (II) complex. J. Am. Chem. Soc. 2000, 122, 6331-6332, DOI: 10.1021/ja001328v.
6. Karlin, K. D.; Tyeklár, Z. Bioinorganic chemistry of copper; Springer Science & Business Media, 2012.
7. Blackman, A. G.; Tolman, W. B. Copper-dioxygen and copper-oxo species relevant to copper oxygenases and oxidases. Struct. Bond. 2000, 97, 179-212, https://doi.org/10.1007/3-540-46592-8.
8. Gerdemann, C.; Eicken, C.; Krebs, B. The crystal structure of catechol oxidase: new insight into the function of type-3 copper proteins. Acc. Chem. Res. 2002, 35, 183-191. DOI: 10.1021/ar990019a.
9. Gentschev, P.; Möller, N.; Krebs, B.: New functional models for catechol oxidases. Inorg. Chim. Acta. 2000, 300, 442-452. https://doi.org/10.1016/S0020-1693(99)00553-8.
10. Neves, A.; Rossi, L. M.; Bortoluzzi, A. J.; Mangrich, A. S.; Haase, W.; Werner, R. Synthesis, structure, physicochemical properties and catecholase-like activity of a new dicopper (II) complex. J. Braz. Chem. Soc. 2001, 12, 747-754. http://dx.doi.org/10.1590/S0103-50532001000600010.

11. Banu, K. S.; Chattopadhyay, T.; Banerjee, A.; Bhattacharya, S.; Suresh, E.; Nethaji, M.; Zangrando, E.; Das, D. Catechol oxidase activity of a series of new dinuclear copper (II) complexes with 3, 5-DTBC and TCC as substrates: syntheses, X-ray crystal structures, spectroscopic characterization of the adducts and kinetic studies. Inorg. Chem. 2008, 47, 7083-7093. DOI: 10.1021/ic701332w.
12. Osório, R. E.; Peralta, R. A.; Bortoluzzi, A. J.; de Almeida, V. R.; Szpoganicz, B.; Fischer, F. L.; Terenzi, H. n.; Mangrich, A. S.; Mantovani, K. M.; Ferreira, D. E. Synthesis, Magnetostructural Correlation, and Catalytic Promiscuity of Unsymmetric Dinuclear Copper (II) Complexes: Models for Catechol Oxidases and Hydrolases. Inorg. Chem. 2012, 51, 1569-1589. DOI: 10.1021/ic201876k.
13. Beyazit, N.; Çatıkkaş, B.; Bayraktar, Ş.; Demetgül, C. Synthesis, characterization and catecholase-like activity of new Schiff base metal complexes derived from visnagin: Theoretical and experimental study. J. Mol. Struct. 2016, 1119, 124-132. https://doi.org/10.1016/j.molstruc.2016.04.047.
14. Mistri, S.; Paul, A.; Bhunia, A.; Manne, R. K.; Santra, M. K.; Puschmann, H.; Manna, S. C. A combined experimental and theoretical investigation on the Cu (II) sensing behavior of a piperazinyl moiety based ligand, and catecholase and biological activities of its Cu (II) complex in combination with pyridine 2, 5-dicarboxylate. Polyhedron 2016, 104, 63-72. https://doi.org/10.1016/j.poly.2015.11.030.
15. Camargo, T. P.; Peralta, R. A.; Moreira, R.; Castellano, E. E.; Bortoluzzi, A. J.; Neves, A. New mononuclear copper (II) complex based on a salen derivative ligand with an unusual coordination and its catecholase activity. Inorg. Chem. Commun. 2013, 37, 34-38. https://doi.org/10.1016/j.inoche.2013.09.039.
16. Stadler, A.-M.; Harrowfield, J.: Bis-acyl-/aroyl-hydrazones as multidentate ligands. Inorganica Chimica Acta 2009, 362, 4298-4314.
17. Konar, S.; Jana, A.; Das, K.; Ray, S.; Golen, J. A.; Rheingold, A. L.; Kar, S. K. A rare pentanuclear cadmium(II) complex and two new mononuclear zinc(II) complexes of pyrazole derived ditopic ligands – Synthesis, crystal structures and spectral studies. Inorg. Chim. Acta. 2013, 397, 144-151. https://doi.org/10.1016/j.ica.2012.12.003.
18. Gokce, C.; Gup, R. Synthesis and characterisation of Cu (II), Ni (II), and Zn (II) complexes of furfural derived from aroylhydrazones bearing aliphatic groups and their interactions with DNA. Chem. Pap. 2013, 67, 1293-1303. https://doi.org/10.2478/s11696-013-0379-8.
19. Salem, N. M. H.; El-Sayed, L.; Foro, S.; Haase, W.; Iskander, M. F. Metal complexes derived from hydrazoneoxime ligands: III – Synthesis, characterization and electrospray ionization mass spectra of some nickel(II) complexes with aroylhydrazoneoximes. Polyhedron 2007, 26, 4161-4172. https://doi.org/10.1016/j.poly.2007.05.010.
20. Naskar, S.; Mishra, D.; Chattopadhyay, S. K.; Corbella, M.; Blake, A. J.: Versatility of 2, 6-diacetylpyridine (dap) hydrazones in stabilizing uncommon coordination geometries of Mn (II): synthesis, spectroscopic, magnetic and structural characterization. Dalton Trans. 2005, 2428-2435. DOI:10.1039/B503891J.
21. Uppadine, L. H.; Lehn, J. M.: Three-Level Synthetic Strategy Towards Mixed-Valence and Heterometallic [2× 2] Gridlike Arrays. Angew. Chem. Int. Ed. 2004, 43, 240-243, doi:10.1002/anie.200352937.
22. Ruben, M.; Lehn, J.-M.; Vaughan, G. Synthesis of ionisable [2× 2] grid-type metallo-arrays and reversible protonic modulation of the optical properties of the [Co II4 L 4] 8+ species. Chem. Commun. 2003, 1338-1339, DOI:10.1039/B303922F.
23. Mondal, S.; Das, C.; Ghosh, B.; Pakhira, B.; Blake, A. J.; Drew, M. G.; Chattopadhyay, S. K. Synthesis, spectroscopic studies, X-ray crystal structures, electrochemical properties and DFT calculations of three Ni (II) complexes of aroyl hydrazone ligands bearing anthracene moiety. Polyhedron 2014, 80, 272-281, https://doi.org/10.1016/j.poly.2014.05.028.
24. He, Z.; He, C.; Gao, E.-Q.; Wang, Z.-M.; Yang, X.-F.; Liao, C.-S.; Yan, C.-H. Lanthanide-transition heterometallic extended structures with novel orthogonal metalloligand as building block. Inorg. Chem. 2003, 42, 2206-2208, DOI: 10.1021/ic026271n.
25. Sakai, K.; Tomita, Y.; Ue, T.; Goshima, K.; Ohminato, M.; Tsubomura, T.; Matsumoto, K.; Ohmura, K.; Kawakami, K. Syntheses, antitumor activity, and molecular mechanics studies of cis-PtCl2(pzH)2 (pzH=pyrazole) and related complexes. Crystal structure of a novel Magnus-type double-salt [Pt(pzH)4][PtCl4][cis-PtCl2(pzH)2]2 involving two perpendicularly aligned 1D chains. Inorg. Chim. Acta. 2000, 297, 64-71, https://doi.org/10.1016/S0020-1693(99)00287-X.

26. Fan, C.; Su, H.; Zhao, J.; Zhao, B.; Zhang, S.; Miao, J. A novel copper complex of salicylaldehyde pyrazole hydrazone induces apoptosis through up-regulating integrin β4 in H322 lung carcinoma cells. Eur. J. Med. Chem. 2010, 45, 1438-1446, https://doi.org/10.1016/j.ejmech.2009.12.048.
27. Abu-Surrah, A. S.; Safieh, K. A. A.; Ahmad, I. M.; Abdalla, M. Y.; Ayoub, M. T.; Qaroush, A. K.; Abu-Mahtheieh, A. M. New palladium (II) complexes bearing pyrazole-based Schiff base ligands: Synthesis, characterization and cytotoxicity. Eur. J. Med. Chem. 2010, 45, 471-475, https://doi.org/10.1016/j.ejmech.2009.10.029.
28. Saha, N. C.; Mandal, S.; Das, M.; Khatun, N.; Mitra, D.; Samanta, A.; Slawin, A. M. Z.; Butcher, R. J.; Saha, R. Synthesis, characterization, X-ray crystallography and antimicrobial activities of new Co(III) and Cu(II) complexes with a pyrazole based Schiff base ligand. Polyhedron 2014, 68, 122-130, https://doi.org/10.1016/j.poly.2013.10.016.
29. Sau, D. K.; Butcher, R. J.; Chaudhuri, S.; Saha, N. Spectroscopic, structural and antibacterial properties of copper (II) complexes with bio-relevant 5-methyl-3-formylpyrazole N (4)-benzyl-N (4)-methylthiosemicarbazone. Mol. Cell. Biochem. 2003, 253, 21-29, https://doi.org/10.1023/A:1026041032078.
30. Kupcewicz, B.; Sobiesiak, K.; Malinowska, K.; Koprowska, K.; Czyz, M.; Keppler, B.; Budzisz, E. Copper (II) complexes with derivatives of pyrazole as potential antioxidant enzyme mimics. Med. Chem. Res. 2013, 22, 2395-2402, https://doi.org/10.1007/s00044-012-0233-5.
31. Mouadili, A.; Attayibat, A.; Kadiri, S. E.; Radi, S.; Touzani, R. Catecholase activity investigations using in situ copper complexes with pyrazole and pyridine based ligands. Appl. Catal., A. 2013, 454, 93-99, https://doi.org/10.1016/j.apcata.2013.01.011.
32. Bouabdallah, I.; Touzani, R.; Zidane, I.; Ramdani, A. Synthesis of new tripodal ligand: N, N-bis [(1, 5-dimethylpyrazol-3-yl) methyl] benzylamine.: Catecholase activity of two series of tripodal ligands with some copper (II) salts. Catal. Commun. 2007, 8, 707-712, https://doi.org/10.1016/j.catcom.2006.08.034.
33. Bouabdallah, I.; Touzani, R.; Zidane, I.; Ramdani, A. Effect of two isomeric tetrapyrazolyl ligands on the catalytic oxidation of 3, 5-di-tert-butylcatechol. J. Iran. Chem. Soc. 2007, 4, 299-303, https://doi.org/10.1007/BF03245978.
34. El Kodadi, M.; Malek, F.; Touzani, R.; Ramdani, A. Synthesis of new tripodal ligand 5-(bis (3, 5-dimethyl-1H-pyrazol-1-ylmethyl) amino) pentan-1-ol, catecholase activities studies of three functional tripodal pyrazolyl N-donor ligands, with different copper (II) salts. Catal. Commun. 2008, 9, 966-969, https://doi.org/10.1016/j.catcom.2007.09.038.
35. Mouadili, A.; Zerrouki, A.; Herrag, L.; Hammouti, B.; El Kadiri, S.; Touzani, R. Catechol oxidation: activity studies using electron-rich nitrogen-based ligands. Res. Chem. Intermed. 2012, 38, 2427-2433, https://doi.org/10.1007/s11164-012-0558-1.
36. Karrouchi, K.; Yousfi, E.; Sebbar, N.; Ramli, Y.; Taoufik, J.; Ouzidan, Y.; Ansar, M. h.; Mabkhot, Y.; Ghabbour, H.; Radi, S. New Pyrazole-Hydrazone Derivatives: X-ray Analysis, Molecular Structure Investigation via Density Functional Theory (DFT) and Their High In-Situ Catecholase Activity. Int. J. Mol. Sci. 2017, 18, 2215, doi:10.3390/ijms18112215.
37. Boussalah, N.; Touzani, R.; Bouabdallah, I.; Kadiri, S. E.; Ghalem, S. Synthesis, structure and catalytic properties of tripodal amino-acid derivatized pyrazole-based ligands. Journal of Molecular Catalysis A: Chemical 2009, 306, 113-117, https://doi.org/10.1016/j.molcata.2009.02.031.
38. Zerrouki, A.; Touzani, R.; El Kadiri, S. Synthesis of new derivatized pyrazole based ligands and their catecholase activity studies. Arab. J. Chem. 2011, 4, 459-464, https://doi.org/10.1016/j.arabjc.2010.07.013.
39. Thabti, S.; Djedouani, A.; Rahmouni, S.; Touzani, R.; Bendaas, A.; Mousser, H.; Mousser, A. Synthesis, X-ray crystal structures and catecholase activity investigation of new chalcone ligands. J. Mol. Struct. 2015, 1102, 295-301, https://doi.org/10.1016/j.molstruc.2015.08.071.
40. Karrouchi, K.; Charkaoui, Y.; Benlafya, K.; Ramli, Y.; Taoufik, J.; Radi, S.; Ansar, M.: Synthesis, characterization and preliminary biological activity of some new pyrazole carbohydrazide derivatives. J. Chem. Pharm. Res. 2013, 5, 1-6.
41. Karrouchi, K.; Ansar, M. h.; Radi, S.; Saadi, M.; El Ammari, L. Crystal structure of N′-diphenylmethylidene-5-methyl-1H-pyrazole-3-carbohydrazide. Acta Crystallogr. E Crystallogr. Commun. 2015, 71, o890-o891, https://doi.org/10.1107/S2056989015020071.

42. Sheldrick, G. A short history of SHELX. Acta Crystallogr. 2008, 64, 112-122, DOI: 10.1107/S0108767307043930.
43. Sheldrick, G. M. Crystal structure refinement with SHELXL. Acta Crystallogr. C. 2015, 71, 3-8, https://doi.org/10.1107/S2053229614024218.
44. BecNe, A. Densityüfunctional thermochemistry. III. The role of exact exchange. J. Chem. Phys 1993, 98, 5648-5652, https://doi.org/10.1063/1.464913.
45. Frisch, M.; Trucks, G.; Schlegel, H. B.; Scuseria, G.; Robb, M.; Cheeseman, J.; Scalmani, G.; Barone, V.; Mennucci, B.; Petersson, G.: Gaussian 09, revision D. 01. Gaussian, Inc., Wallingford CT, 2009.
46. Becke, A. D.: Density-functional exchange-energy approximation with correct asymptotic behavior. Phys. Rev. 1988, 38, 3098, DOI:https://doi.org/10.1103/PhysRevA.38.3098.

Sample Availability: Samples of the compounds ..... are available from the authors.